

# Spontaneous growth of freestanding Ga nanoribbons from Cr<sub>2</sub>GaC surfaces

Zheng Ming Sun<sup>a)</sup>

*Department of Materials Science and Engineering, Drexel University, Philadelphia, Pennsylvania 19104; and National Institute of Advanced Industrial Science and Technology (AIST), Nagoya 463-8560, Japan*

Surojit Gupta, Haihui Ye, and Michel W. Barsoum

*Department of Materials Science and Engineering, Drexel University, Philadelphia, Pennsylvania 19104*

(Received 28 March 2005; accepted 28 June 2005)

Herein we report on the room-temperature spontaneous growth of Ga freestanding nanoribbons from Cr<sub>2</sub>GaC surfaces. An oxidation-based model is proposed to explain the growth of the nanostructures. The nanoribbons present a unique opportunity to study the behavior of electrons confined to two dimensions. The production of these Ga nanostructures could be the first step in the manufacture of gallium arsenide or nitride devices with enhanced characteristics for photonic, electronic, and catalytic applications.

Nanoribbons have recently attracted some attention due to their potential application in photonics and electronics. These reports have mainly focused on oxides such as ZnO,<sup>1,2</sup> gallium nitride,<sup>3,4</sup> fullerenes C<sub>60</sub>,<sup>5</sup> and the semiconductor Se.<sup>6,7</sup> As far as we are aware, there is no report on metal-based nanoribbons in the literature. In this work, we report on our discovery of the spontaneous growth of Ga-based freestanding nanoribbons from polished and fractured surfaces of the ternary compound Cr<sub>2</sub>GaC.

Predominantly single-phase samples of Cr<sub>2</sub>GaC, containing ~1 vol% free Ga, uniformly distributed along the grain boundaries were fabricated. Commercial Cr powder (99.99%, -325 mesh), graphite powder (99%, -300 mesh), and Ga pellets (99.99%, 3 mm) (all from Alpha Aesar, Ward Hill, MA) were mixed in stoichiometric proportions, ball milled for 1 h, and sealed in borosilicate glass tubes under mechanical vacuum. The tubes were heated to 650 °C for 10 h, which resulted in their collapse and allowed the powders to pre-react. The tubes were placed in a hot isostatic press heated at 10 °C/min to 650 °C, followed by heating at 2 °C/min to 750 °C. The chamber was pressurized with Ar gas to 70 MPa, further heated at 10 °C/min to 1200 °C, and held at temperature for 12 h.

Differential scanning calorimetry measurements established the presence of ~1 vol% Ga.<sup>8</sup> From the fractured surfaces, the Ga thickness between grains was estimated

to be ~0.1 μm. Polished and fracture surfaces were observed with a scanning electron microscope (SEM; FEI, XL30S, Hillsboro, OR) equipped with an energy dispersive spectrum (EDS) analyzer and an electron backscattering patterns (EBSP) detector. A JEOL 2010F (Tokyo, Japan) transmission electron microscope (TEM) with FasTEM control system, operated at 200 kV, with a point-to-point resolution of 0.23 nm, was used for TEM analysis. An in situ TEM video was recorded to demonstrate the motion of liquid Ga under the electron beam.

Figures 1 and 2 show a collection of nanoribbons in SEM micrographs with various morphologies observed on polished (Fig. 1) and fractured (Fig. 2) surfaces. The majority of nanoribbons were freestanding and appeared to grow, more or less, normal to the Cr<sub>2</sub>GaC basal planes [Figs. 1(a), 1(b), 1(c), 1(h), 2(a), 2(b)]. Cr<sub>2</sub>GaC is hexagonal and the grains tend to grow along the basal planes, resulting in thin platelike grains. The resulting structures were reminiscent of grass swaying in water [Fig. 2(b)] or a wisp of smoke. In some cases, the nanoribbons appear to be peeling off the Cr<sub>2</sub>GaC basal planes [Figs. 2(a) and 2(c)].

These nanoribbons must be exceedingly thin because they are transparent to both secondary and backscattered SEM electrons [Figs. 1(c), 1(f)–1(i), 2(a), 2(c)]. Viewed edge-on [Fig. 1(e)] their thickness was estimated to be at most 10 nm. According to electron backscattered diffraction (EBSD), the nanoribbons were either amorphous or nanocrystalline. Their volume could also be insufficient to produce a measurable signal. When viewed in the TEM [Fig. 3(a)], however, the images started moving, indicating the presence of a fluid. Notably, this fluid—assumed to be molten Ga—did not spill out, or spheroidize,

<sup>a)</sup>Address all correspondence to this author.

e-mail: z.m.sun@aist.go.jp  
DOI: 10.1557/JMR.2005.0326

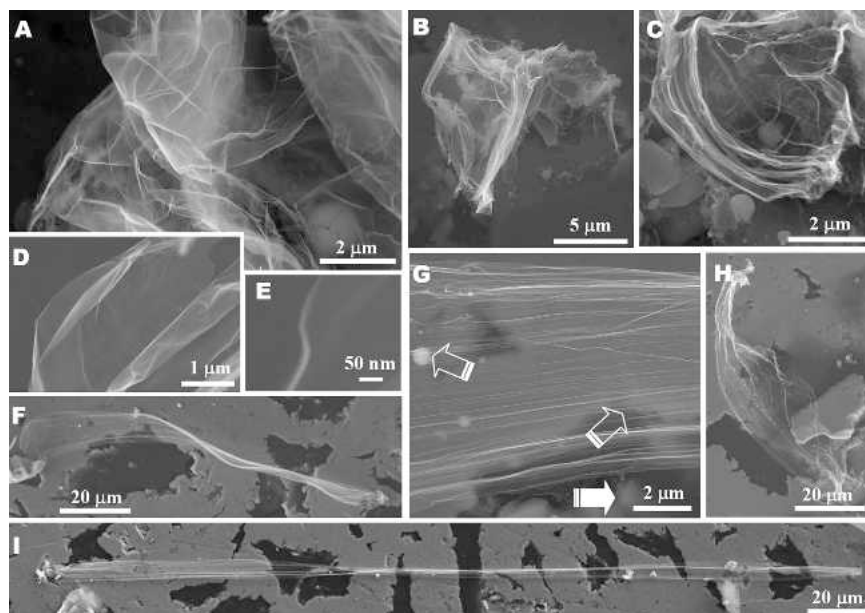


FIG. 1. Typical SEM micrographs taken on polished surfaces of  $\text{Cr}_2\text{GaC}$  showing: (a–c) freestanding nanoribbons normal to the surface, (d, e) edge-on observations of the nanoribbons showing thickness of less than 10 nm. (f, h, i) long nanoribbons laying on the surface of the sample [ $a \sim 280\ \mu\text{m}$  in (i)], (g) selected raster from (f) showing the transparency of the nanoribbon. Dark regions show where grains were pulled out and replaced by diamond suspension used for polishing. Note transparency of nanoribbons.

strongly suggesting it is contained in an oxide skin. Consistent with this view is the fact that the ridge seen at the bottom of the micrograph—which we presume it to be part of the oxide skin—did not “melt” or move with time. After a few minutes under the beam, the image stopped “moving” and high-resolution TEM micrographs indicated the presence of lattice planes, with a spacing of  $\sim 2.8\ \text{\AA}$  [Fig. 3(b)], that we believe are Ga (102) planes. It thus appears that exposure to the electron beam resulted in the solidification and crystallization of the Ga in the ribbons. The fact that Ga has a strong tendency to supercool—by as much as 35 K in some cases—is fully consistent with our findings.<sup>9,10</sup>

In the remainder of this paper, we propose a model for the growth of the nanoribbons. When, upon fracture, a pre-existing Ga layer—or one that spreads onto the basal

planes as a result of fracture [Fig. 4(a)]—is exposed to oxygen, this layer rapidly oxidizes to form an ultrathin outer oxide skin. What follows is believed to depend on the rate at which the Ga arrives to the growing surface. If the Ga flux is rapid, microbundles (not shown here) are observed to grow normal to the  $\text{Cr}_2\text{GaC}$  basal planes. If the Ga flux to the surface is slow or limited, oxygen diffusion down the Ga/ $\text{Cr}_2\text{GaC}$  interface results in the formation of a second skin that encapsulates the Ga into a ribbon [Fig. 4(b)]. In most cases, this causes the ribbons to dewet and stand freely [right hand side, Fig. 4(b)]. Direct evidence for dewetting can be seen in Fig. 2(c) and its inset. To produce the  $\sim 280\text{-}\mu\text{m}$ -long ribbon shown in Fig. 1(i), the ribbon would have had to grow parallel to the surface [left side in Fig. 4(b)].

Because the ribbons are no longer wetting the basal

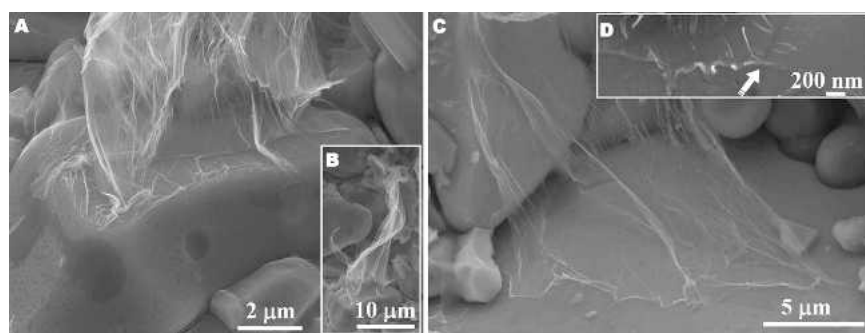


FIG. 2. Typical SEM micrographs taken on the fracture surface of  $\text{Cr}_2\text{GaC}$  showing (a) freestanding nanoribbons and (b) the overall image of the nanoribbons at lower magnification, (c) a large sheet of nanoribbons dewetting from the basal plane of a grain on the fracture surface, and (d) the dewetting from grain surface and fracture of a nanoribbon (arrow).

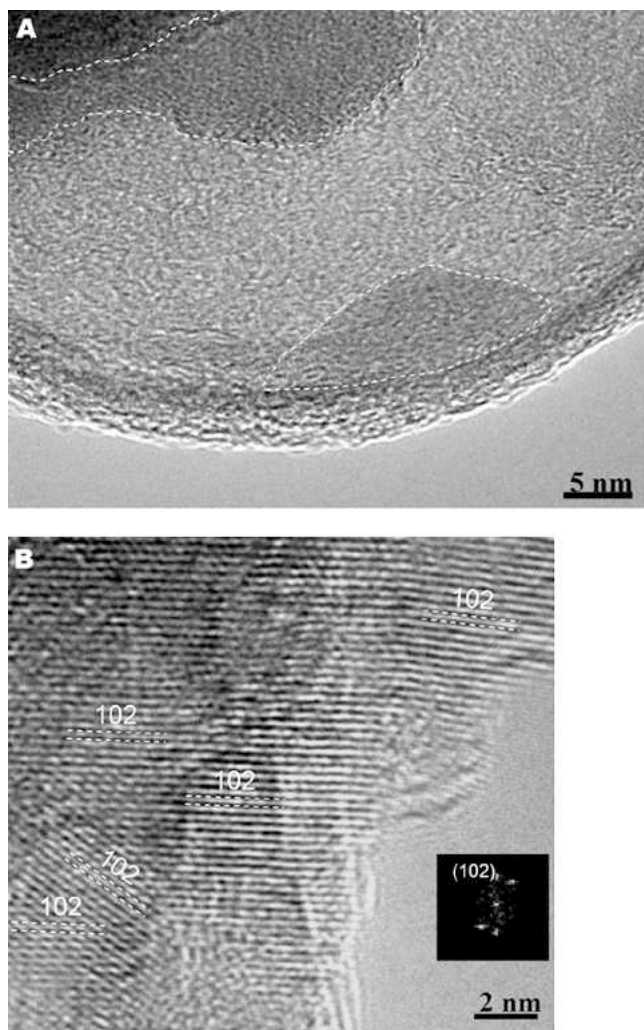


FIG. 3. Typical high-resolution TEM micrographs of a nanoribbon: (a) observed to “boil” under the electron beam without spheroidizing. The dark contrast areas marked with dashed lines are the fluid areas, which eventually transform to look like the light grey areas. The bottom ridge was stable under the electron beam. (b) After  $\sim 2$  min under the electron beam, the formation of Ga nanocrystals was observed. Inset is the fast Fourier transform (FFT) diffraction pattern converted from the high-resolution fringe image.

planes, the driving force for their continued growth cannot be surface energy reduction. In that case, the most likely driving force is oxidation. We also note that while the ribbon is growing at its base, the oxide skin must be forming on the same time scale and conforming to it.

The following observations are consistent with our model. At  $\sim 0.98$  of its melting point (MP) and the huge Ga surface areas involved, it is remarkable that the nanoribbons do not spheroidize. This observation is crucial and implies that the increase in surface energy is more than compensated for by other means. It also implies the presence of a potent inhibitor to sintering/spheroidization, etc. We believe that the thin Ga oxide layer formed is key. The free-energy changes for oxidation are typically

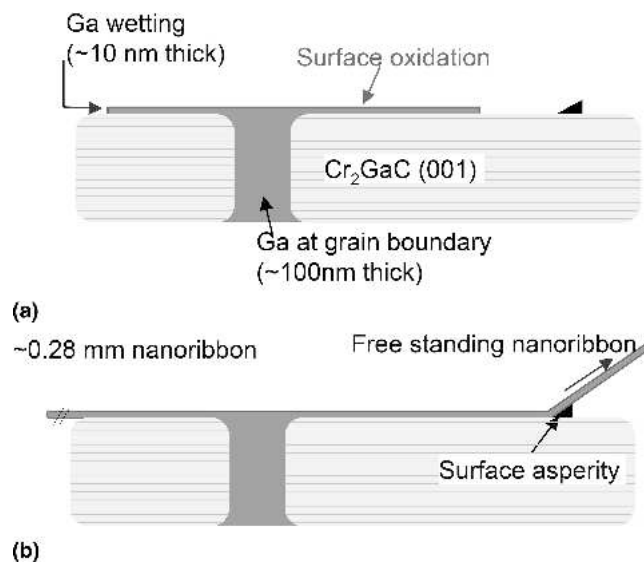


FIG. 4. Schematic illustration outlining the spontaneous growth of nanoribbons: (a) upon fracture, the basal planes are covered by a thin Ga film that, in turn, is rapidly covered by a thin oxide layer; (b) oxidation of the underside of the Ga film results in nanoribbons that either grow parallel to the surface (left-hand side) or become freestanding (right-hand side).

two orders of magnitude greater than those for sintering.<sup>11</sup> We thus postulate that the driving force for the growth of nanoribbons is essentially an oxidation reaction. In other words, Ga–Ga bonds are replaced by Ga–O bonds. (At 25 °C, the heat of formation of  $\beta$ -Ga<sub>2</sub>O<sub>3</sub> is  $\sim 1080$  kJ/mol). Note Ga rapidly forms Angstrom-thick oxide films at room temperature.<sup>12</sup> Along the same lines, we have recently shown that oxidation is responsible for the spontaneous growth of soft metal (e.g., In, Sn, Pb, etc.) whiskers, solving a 50+ year old mystery.<sup>13,14</sup>

The fact that passing a TEM electron beam through the nanoribbons does not melt but solidifies them is remarkable and implies extremely high rates of heat transfer which must be related to the enormous surface-to-volume ratios involved and their freestanding nature. The thermal conductivity of Ga along the *b*-axis is 88 W/mK.<sup>15</sup>

It is nontrivial to obtain freestanding, non-planar ultrathin films of metals, especially supercooled ones. Herein we show that such films can be grown, rather easily, in lateral dimensions that are easy to work with. Consequently, the nature of the liquid to solid transition—confined to two dimensions—and its effect on properties can now be experimentally explored.

Lastly we note that Cr<sub>2</sub>GaC is but one of a family of 50+ ternary compounds, the M<sub>n+1</sub>AX<sub>n</sub> (MAX) phases (where M is an early transition metal, A an A-group element, X carbon or nitrogen, *n* = 1 to 3).<sup>16</sup> It is thus possible that freestanding nanoribbons of Al, As, In, Sn, and Pb, among others can be grown at room or slightly higher temperatures. If the physics holds at even higher temperatures, it may even be possible to template and

grow Si and Ge nanoribbons. These comments notwithstanding, it is clear that more work is needed to better understand and control the growth of the structures described herein.

## ACKNOWLEDGMENTS

This work was funded by the Office of Naval Research (ONR; N00421-03-C-0085) and National Science Foundation (NSF; DMR 0072067). We would also like to thank Prof. R. Doherty of Drexel University for many stimulating discussions.

## REFERENCES

1. M. Law, D.J. Sirbuly, J.C. Johnson, J. Goldberger, R.J. Saykally, and P. Yang: Nanoribbon waveguides for subwavelength photonics integration. *Science* **305**, 1269 (2004).
2. X. Kong and Y. Li: High sensitivity of CuO modified SnO<sub>2</sub> nanoribbons to H<sub>2</sub>S at room temperature. *Sens. Actuators, B* **105**, 449 (2005).
3. L. Yang, X. Zhang, R. Huang, G. Zhang, and X. An: Synthesis of single crystalline GaN nanoribbons on sapphire (0001) substrates. *Solid State Commun.* **130**, 769 (2004).
4. X. Xiang, C. Cao, F. Huang, R. Lv, and H. Zhu: Synthesis and characterization of crystalline gallium nitride nanoribbon rings. *J. Cryst. Growth* **263**, 25 (2004).
5. M. Nakaya, T. Nakayama, and M. Aono: Fabrication and electron-beam-induced polymerization of C<sub>60</sub> nanoribbon. *Thin Solid Films* **464-465**, 327 (2004).
6. H. Zhang, M. Zuo, S. Tan, G. Li, S. Zhang, and J. Hou: Carbo-thermal chemical vapor deposition route to Se one-dimensional nanostructures and their optical properties. *J. Phys. Chem. B* **109**, 10653 (2005).
7. X.B. Cao, Y. Xie, S.Y. Zhang, and F.Q. Li: Ultrathin trigonal selenium nanoribbons developed from series-wound beads. *Adv. Mater.* **16**, 649 (2004).
8. T. El-Raghy, S. Chakraborty, and M.W. Barsoum: Synthesis and characterization of Hf<sub>2</sub>PbC, Zr<sub>2</sub>PbC, and M<sub>2</sub>SnC (M = Ti, Hf, Nb or Zr). *J. Eur. Ceram. Soc.* **20**, 2619 (2000).
9. M. Hida, A. Sakakibara, and H. Kamiyabu: Surface tension and supercooling phenomenon of liquid Ga. *J. Jpn. Inst. Met.* **53**, 1263 (1989).
10. Z. Liu, Y. Bando, M. Mitome, and J. Zhan: Unusual freezing and melting of gallium encapsulated in carbon nanotubes. *Phys. Rev. Lett.* **93**, 095504-1 (2004).
11. M.W. Barsoum: *Fundamentals of Ceramics* (Institute of Physics, Bristol, U.K., 2003), p. 331.
12. M.J. Regan, H. Tosmann, P.S. Pershan, O.M. Magnussen, E. DiMasi, B.M. Ocko, and M. Deutsch: X-ray study of the oxidation of liquid-gallium surfaces. *Phys. Rev. B* **55**, 10786 (1997).
13. M.W. Barsoum, E.N. Hoffman, R.D. Doherty, S. Gupta, and A. Zavaliangos: Driving force and mechanism for spontaneous setal whisker formation. *Phys. Rev. Lett.* **93**, 206104-1 (2004).
14. Z.M. Sun and M.W. Barsoum: Spontaneous room temperature extrusion of Pb nano-whiskers from leaded brass surfaces. *J. Mater. Res.* **20**, 1087 (2005).
15. D.R. Lide: *CRC Handbook of Chemistry and Physics*, 85th ed. (CRC Press Inc., Boca Baton, FL, 2004), pp. 150, 285.
16. M.W. Barsoum: The M<sub>N+1</sub>AX<sub>N</sub> phases: A new class of solids: Thermodynamically stable nanolaminates. *Prog. Solid State Chem.* **28**, 201 (2000).